in vivo *38*: 1170-1181 (2024)
doi:10.21873/invivo.13552

Box A of HMGB1 Maintains the DNA Gap and Prevents DDR-induced Kidney Injury in D-galactose Induction Rats

WILUNPLUS KHUMSRI[1,2], WITCHUDA PAYUHAKRIT[3,4], APHISEK KONGKAEW[5], NIPON CHATTIPAKORN[6,7], SIRIPORN CHATTIPAKORN[6,8], SAKAWDAURN YASOM[1] and APIWAT MUTIRANGURA[1]

[1]*Center of Excellence in Molecular Genetics of Cancer and Human Disease, Department of Anatomy, Faculty of Medicine, Chulalongkorn University, Bangkok, Thailand;*
[2]*Interdisciplinary Program of Biomedical Sciences, Graduate School, Chulalongkorn University, Bangkok, Thailand;*
[3]*Department of Pathobiology, Faculty of Science, Mahidol University, Bangkok, Thailand;*
[4]*Pathobiology Information and Learning Center, Department of Pathobiology, Faculty of Science, Mahidol University, Bangkok, Thailand;*
[5]*Research Administration Section, Faculty of Medicine, Chiang Mai University, Chiang Mai, Thailand;*
[6]*Center of Excellence in Cardiac Electrophysiology Research, Chiang Mai University, Chiang Mai, Thailand;*
[7]*Cardiac Electrophysiology Unit, Department of Physiology, Faculty of Medicine, Chiang Mai University, Chiang Mai, Thailand;*
[8]*Neurophysiology Unit, Cardiac Electrophysiology Research and Training Center, Faculty of Medicine, Chiang Mai University, Chiang Mai, Thailand*

Abstract. *Background/Aim: Disability and mortality rates for renal failure are still increasing. DNA damage and oxidative stress intoxication from body metabolism, high blood glucose, or the environment cause significant kidney damage. Recently, we reported that Box A of HMGB1 (Box A) acts as molecular scissors, producing DNA gaps that prevent DNA damage in kidney cell lines and ultimately reverse aging phenotypes in aging rat models. The present study aimed to demonstrate the potency of Box A in preventing D-galactose (D-gal)-induced kidney injury. Materials and Methods: A Box A expression plasmid was constructed and administered to a rat model. D-gal was injected subcutaneously for eight weeks. Serum was collected to study renal function, and white blood cells were collected for DNA gap measurement. Kidney tissue was also collected for γ-H2AX and NF-κB immunostaining; Senescence-associated (SA)-beta-gal staining; and analysis of the mRNA expression of $p16^{INK4A}$, TNF-α, and IL-6. Moreover, histopathology analysis was performed using hematoxylin & eosin and Masson trichome staining. Results: Pretreatment with Box A administration prevented the reduction of DNA gaps and the consequences of the DNA damage response, which include elevated serum creatinine; high serum BUN; an increased positive SA-beta-gal staining area; overexpression of $p16^{INK4A}$, NF-κB and senescence-associated secretory phenotype molecules, including IL-6, TNF-α; and histological alterations, including tubular dilation and collagen accumulation. Conclusion: Box A effectively prevents DNA gap reduction and all D-gal-induced kidney pathological changes at the molecular, histological, and physiological levels. Therefore, Box A administration is a promising novel therapeutic strategy to prevent DNA-damaging agent-induced kidney failure.*

Correspondence to: Witchuda Payuhakrit, Department of Pathobiology, Faculty of Science, Mahidol University, Bangkok, Thailand. E-mail: witchuda.pay@mahidol.ac.th; Sakawdaurn Yasom, Center of Excellence in Molecular Genetics of Cancer and Human Disease, Department of Anatomy, Faculty of Medicine, Chulalongkorn University, Bangkok, Thailand. E-mail: sakawdaurn.y@chula.ac.th

Key Words: Kidney failure, DNA protection, DNA damage, DNA durability, Box A of HMGB1, youth-DNA gap.

DNA damage and the associated DNA damage response (DDR) have been identified as common causes of kidney injury. Chemicals, ischemia-reperfusion injury, or sepsis can cause DNA damage with increased apoptosis of renal tubular epithelial cells, interstitial fibrosis, and ultimately chronic kidney disease (CKD) (1). Diabetes is a critical and commonly leading cause of CKD that accounts for nearly 50% of the

incidence of end-stage kidney disease, which is considered the most severe type of kidney injury. Diabetes Mellitus (DM) is responsible for increased mortality of patients with kidney diseases (2). One of the most prominent kinds of DNA damage implicated in the pathological process of kidney injury is reactive oxygen species (ROS)-induced oxidative stress-driven DNA damage (3). In oxidative stress models, D-galactose (D-gal) is frequently utilized as an inducer. Prolonged administration of D-gal to rats can result in oxidative stress, inflammation, and DNA damage, all of which lead to renal injury (4, 5) through the DDR signaling pathway (6).

For over a decade, our group has studied a new epigenetic mark called a youth-associated genomic stabilization DNA gap (youth-DNA-gap or DNA gap) or a replication-independent endogenous DNA double-strand break (RIND-EDSB) (7-12). The role of Box A of HMGB1 in enhancing stem cell properties of human mesenchymal cells (13) was published by our group. Recently, we also reported that decreased youth-DNA-gap numbers were observed in patients with type 2 DM and associated with increased HbA1c levels (14). The DNA gap complex is composed of Box A of high mobility group Box 1 protein (Box A), which produces a DNA gap, Sirtuin 1 (SIRT1), which deacetylates histones, and Argonaute RISC component 4 (AGO4), which methylates DNA (15, 16). DNA gaps play a role in DNA protection and promote genomic stability by relieving the DNA torsion force due to double-helix denaturation during transcription or replication (10). Alterations or reductions in DNA gaps have been reported to promote genomic instability during chronological aging (10, 15). However, a previous study has shown that Box A-produced DNA gaps have protective roles in genomic stabilization, preventing DNA damage and DDR *via* many signaling pathways such as by decreasing the levels of the variant histone H2AX (γ-H2AX) and enhancing the stability of produced DNA gaps (10, 15). Furthermore, hypermethylation that predominates in young cells can be observed in DNA sequences near Box A-produced DNA gaps (16, 17). Hence, Box A-produced DNA gaps could be effective therapeutic targets for preventing kidney injury caused by DNA damage and the DDR.

Attenuation of renal injury has become essential. Currently, the pharmacological strategies for renal injury include modulating epigenetic alterations (18), combating fibrosis (19), reducing senescence (20), and targeting autophagic activity (21). All of those pharmacological strategies principally act on the consequences of persistent DDR-inducing kidney damage. However, disability and mortality due to renal injury are still increasing. Accordingly, it is crucial to discover a novel and more effective target for preventing renal injury, especially for preventing DNA damage. In the present study, we investigated the ability of Box A to prevent kidney injury in D-gal-treated rats. The findings illustrate Box A's potency for prevention and suggest that Box A can be further developed into a novel treatment to ameliorate kidney injury.

Materials and Methods

Plasmid construction. In this study, we used the plasmid DNA of Box A and pcDNA™ 3.1(+) (Addgene, Cambridge, MA, USA), as a plasmid control (PC). The sequence of Box A plasmid is acquired from Gene ID: 3146 (NCBI) and is shown in Table I. We transformed the plasmid DNA into Escherichia coli (DH5α) (Thermo Fisher Scientific, Waltham, MA, USA), specifically, NEB® 5-alpha competent E. coli (New England Biolabs, Beverly, MA, USA). The transformed cells were grown on LB agar with ampicillin for plasmid selection. A selected colony was cultured in LB broth with 100 μg/ml ampicillin and incubated in an incubator shaker at 37˚C for 16 h. After a selective bacterial culture, the plasmids were extracted and purified using a GeneJet Plasmid Maxiprep Kit (Thermo Fisher Scientific) according to the manufacturer's instructions. Sequence fidelity was confirmed by Sanger sequencing (15). The plasmid (5 μg) was then coated with 100 μL of nanoparticle solution and mixed with calcium solution (Merck Millipore, Billerica, MA, USA), a plasmid DNA binding reagent. The plasmid DNA–calcium complex was added to a mixture of sodium carbonate (Merck Millipore) and sodium dihydrogen phosphate monohydrate (Merck Millipore). Finally, nanoparticle-coated plasmids were freshly prepared before use. All steps of nanoparticle solution preparation and plasmid DNA coating were performed using sterile techniques (15).

Animal study. All animal procedures were reviewed and approved by the Animal Care and Use Committee, Chiang Mai University, Thailand, Approval No. 2562/RT0013. All animals were housed in a temperature-controlled chamber (25±0.5˚C) with a 12:12-hour light/dark cycle. Standard diet and sterilized water were provided ad libitum. Eighteen male Wistar rats were used in this study and randomly assigned to three subgroups. The control group contained PC+ normal saline solution (NSS)-treated rats (n=6), the PC+ D-gal group (n=6) was the kidney injury induction group, and the Box A+ D-gal group (n=6) was the group pretreated with Box A before D-gal-induced kidney injury. The PC+NSS and PC+ D-gal groups were intraperitoneally injected with 100 μg of pcDNA3.1 per kg body weight. In contrast, Box A+ D-gal rats were intraperitoneally injected with 100 μg of Box A per kg body weight. Then, after three days, the PC+ D-gal and Box A+ D-gal groups of rats were subcutaneously injected with D-gal (150 mg/kg, Sigma-Aldrich, St. Louis, MO, USA) in NSS daily for eight weeks. The PC+NSS group of rats was administered NSS without D-gal in the same manner. The plasmid DNA was injected into each group once a week for eight weeks. At the end of the treatment, rats from each group were selected and sacrificed by an overdose of anesthetic drug (Isoflurane) inhalation after the last administration (two days after administration). Peripheral serum samples were collected, and kidney rat tissues were immediately collected in 4% paraformaldehyde (PFA) (Sigma-Aldrich), 10% formalin buffer, and RNA storage reagent (Tiangen Biotech, Beijing, PR China) for subsequent analyses.

Detection of serum creatinine and BUN levels in the peripheral blood. Rats from each group were selected (n=5) and sacrificed after the last administration. Peripheral serum samples were collected, and the serum samples were shipped to the Hematology and Biochemistry Laboratory, Small Animal Hospital, Faculty of Veterinary Medicine, Chiang Mai University, for detection of the levels of creatinine and blood urea nitrogen (BUN).

Table I. *The sequence of Box-A of HMGB1 of 285 bp*.

Name	Sequence
Box A of HMGB1	ATGACCATGGACTACAAGGACGACGATGACAAGCTGCAGGAATTCATGGGCAAAGGAGATCCTAAGAAGCCGA GAGGCAAAATGTCATCATATGCATTTTTTGTGCAAACTTGTCGGGAGGAGCATAAGAAGAAGCACCCAGATGCT TCAGTCAACTTCTCAGAGTTTTCTAAGAAGTGCTCAGAGAGGTGGAAGACCATGTCTGCTAAAGAGAAAGGAA AATTTGAAGATATGGCAAAGGCGGACAAGGCCCGTTATGAAAGAGAAATGAAAACCTATATCTAAGTCGACGC GTCTGCAGAAGCTTCTAGAGGGCCCTATTCTATAGTGTCACCTAAAT

Table II. *Primers used in this study.*

Organism	Gene name	Sequence	Reference
Rattus norvegicus	GAPDH	FW 5'-GTATTGGGCGCCTGGTCACC-3' RW 5'-CGCTCCTGGAAGATGGTGATGG-3'	(25)
	$p16^{INK4A}$	FW 5'-GTCAAAGTGGCAGCTCTCCTGCT-3' RW 5'-TGTCGGTGACCCGGGAAACGTTC-3'	(27)
	IL-6	FW 5'TCCTACCCCAACTTCCAATGCTC-3' RW 5'TTGGATGGTCTTGGTCCTTAGCC-3'	(25)
	TNF-α	FW 5'-AAATGGGCTCCCTCTCATCAGTTC-3' RW 5'-TCTGCTTGGTGGTTTGCTACGAC-3'	(25)

High-molecular-weight DNA (HMWDNA) for DNA-GAP measurement. DNA-GAP PCR or IRS-EDSB-LM-PCR was performed as previously reported (12). To assess EDSBs in white blood cells, HMWDNA was obtained for DNA-GAP PCR by using a QuantStudio™ 6 Flex Real-Time PCR system (Thermo Fisher Scientific). The PCR components were 1× TaqMan™ Universal PCR Master Mix (Applied Biosystems, Carlsbad, CA, USA), 0.5 U of HotStarTaq DNA polymerase (Qiagen, Hilden, Germany), 0.3 μM probe homologous to the 3'-linker sequence (6-fam) ACGTCCACGAGGTAAGCTTCCGAGCGA (tamra) (phosphate), 0.5 μM of rat interspersed repetitive sequence (B1) primer (5'-AATCCGCCTGCCTCTGCCTCC-3'), 0.5 μM linker primer (5'-AGGTAACGAGTCAGACCACCGA-3'), and 40 ng of HMWDNA. Control DNA was digested with EcoRV and AluI (Thermo Fisher Scientific) and ligated with linkers to generate a standard curve. The PCR program was as follows: 1 cycle of 50˚C for 2 min followed by 95˚C for 10 min and 60 cycles of 95˚C for 15 s along with 60˚C for 2 min. The number of DNA-GAPs was calculated from a standard curve of control DNA and is reported as the %DNA-GAP PCR, which was calculated *via* the following equation: 100 times the experimental group divided by the control group (%DNA-GAP number of PC+NSS group) (15).

Senescence-associated beta-galactosidase (SA-beta-gal) staining in kidney tissue. After euthanasia, kidney rat tissues were immediately dissected and fixed in fresh fixative buffer. For Senescence-associated (SA)-beta-gal staining of kidney cryosections, tissues were stored in 4% PFA before embedding at the optimum cutting temperature (OCT) compound (Sakura, Tissue-Tek) and cryosectioned at 5 μm thickness. After rehydration of the kidney sections in PBS, the sections were SA-beta-gal-stained using a Cell Signaling Kit (9860; Beverly, MA, USA) with a 15 min fixation followed by 37˚C incubation in the staining solution for 18 h. Five fields were randomly captured (200× magnification) under light microscopy (DM1000; Leica Microsystems, Wetzlar, Germany). The SA-beta-gal-positive area (blue color) was quantified using ImageJ software (National Institutes of Health, Bethesda, Maryland, USA) (22). Two examiners performed the quantitative analysis of the SA-beta-gal-positive area.

Hematoxylin & Eosin staining and Masson trichrome staining. For histopathological analyses, the kidney tissues were fixed in 10% formalin buffer for at least 48 h. Then, the tissue was processed, paraffin-embedded, and sectioned at a thickness of 5 μm. Subsequently, the kidney sections were stained with H&E and Masson trichrome according to standard procedures for histopathological analysis. The histopathological changes were observed and quantitatively analyzed by two examiners under a light microscope (Nikon ECLIPSE). Five fields were randomly selected (100× magnification), photographed with a digital camera (Nikon Digital Sight 10) using NIS-Elements software at maximum resolution and measured for their mean percentages of positive area of tubular dilation (H&E staining) and collagen accumulation (Masson trichrome) using ImageJ software (23).

Immunohistochemical staining. All kidney tissue samples were processed using standard methods, and serial sections were used for immunohistochemistry (IHC), including dewaxing, rehydration, and retrieval using 10 mM sodium citrate buffer (pH 6.0) for 30 min. The sections were then rinsed in PBS, and hydrogen peroxide and BSA were applied to block endogenous peroxidase activity and nonspecific background, respectively. The sections were incubated with anti-γ-H2AX (phospho-S139, AB26350, Abcam, Waltham, MA, USA) and anti-NF-κB p65 (AB16502, Abcam) antibodies at 4˚C overnight. The slides were washed with PBS and incubated with the secondary HRP-conjugated antibody (1:500) for 45 min. The slides were then washed in PBS and incubated with DAB Substrate (Merck) for 30 min at room temperature, and hematoxylin was used for counterstaining.

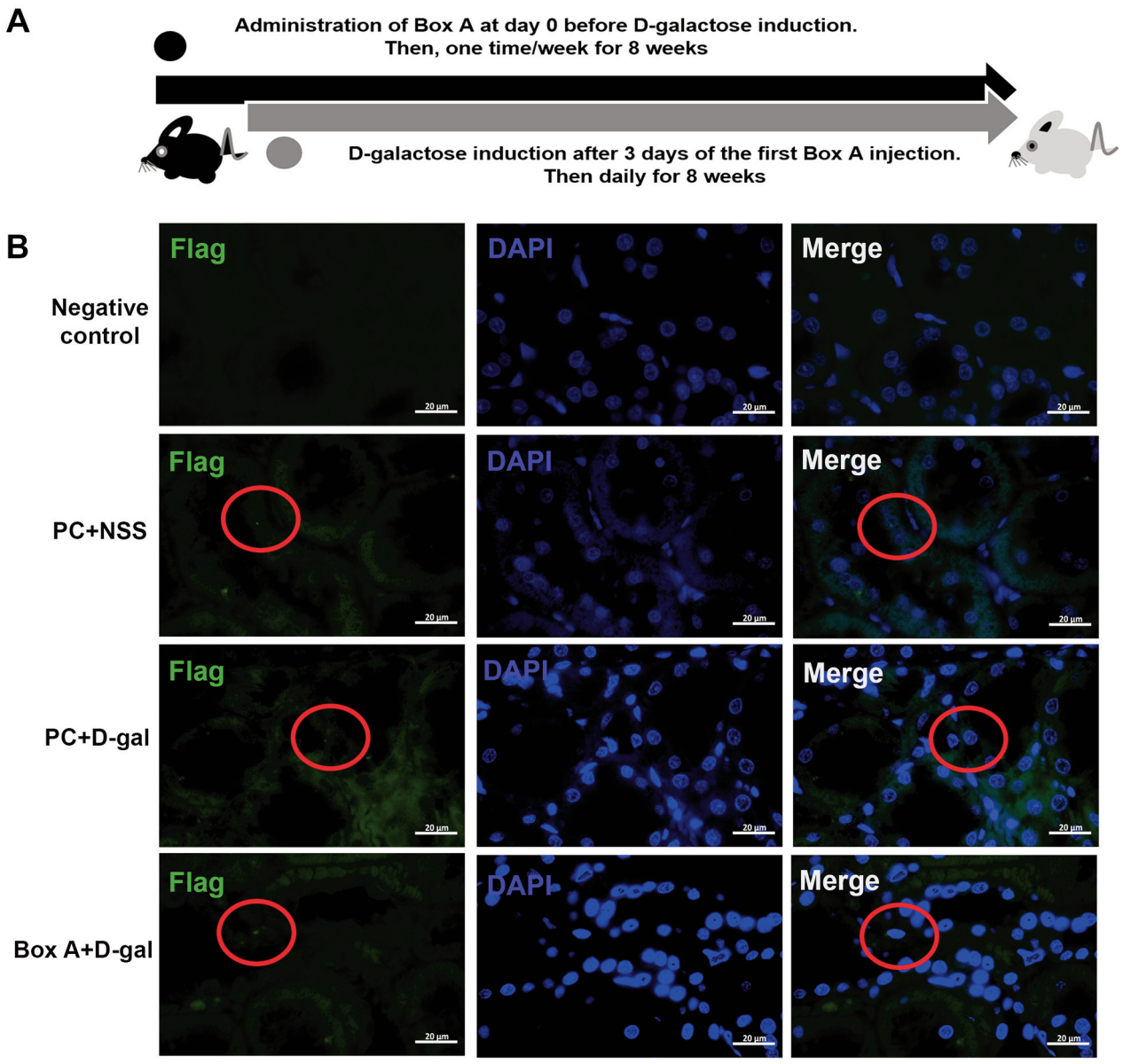

Figure 1. *Continued*

Finally, the slides were observed under a light microscope (Nikon ECLIPSE). Five fields were randomly selected and photographed with a digital camera (Nikon Digital Sight 10) using NIS-Elements software at maximum resolution and measured for their mean percentages of γ-H2AX-positive cells (400× magnification) and percentages of positive area of NF-κB at 400x magnification using ImageJ software (24). Two examiners performed the quantitative analysis of γ-H2AX and NF-κB protein expression.

Immunofluorescence staining. All kidney tissue samples were processed using standard methods, and serial sections were used for an indirect immunofluorescence assay (IFA), which included dewaxing, rehydration, and retrieval using 10 mM sodium citrate buffer (pH 6.0) for 30 min. The sections were then rinsed in PBS. Subsequently, the tissues were permeabilized with PBS containing 0.25% Triton X-100 for 10 min, and PBS containing 5% BSA was applied to block nonspecific background staining for 1 h. The sections were incubated with an anti-DDDDK tag antibody, which binds to the FLAG tag sequence (AB1162, Abcam) (1:100), at 4˚C overnight. The slides were washed with PBS and incubated with fluorescein-conjugated secondary antibody (1:500) for 30 min. DAPI was used for counterstaining. The slides were washed with PBS and mounted using 50% glycerin in PBS. Finally, the slides were observed under a fluorescence microscope (Nikon ECLIPSE) and photographed with a digital camera (Nikon Digital Sight 10) using NIS-Elements software at maximum resolution.

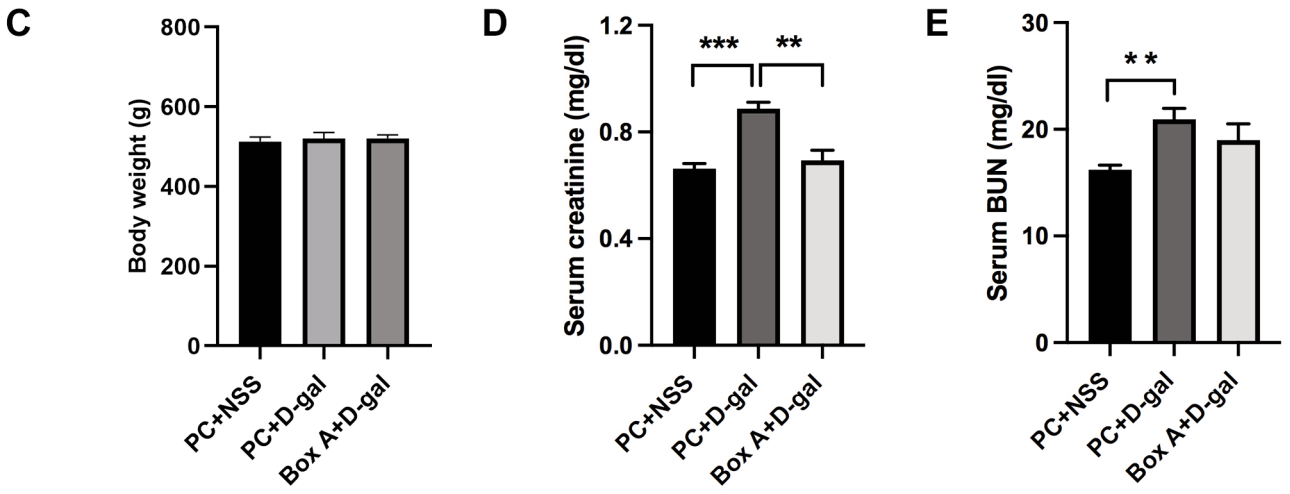

Figure 1. *Preventive effects of Box A on serum renal function in rats with D-gal-induced kidney injury. (A) Schematic diagrams for the groups pretreated with Box A plasmid/Ca-P nanoparticle (Box A) (100 μg/kg/week, i.p.) or PC/Ca-P nanoparticle (100 μg/kg/week, i.p.) on Day 0 and then treated daily with D-galactose (150 mg/kg/day, s.c.) beginning three days later and continuing for eight weeks. (B) The FLAG tag sequence was detected using immunofluorescence staining for representative plasmid delivery, represented in a green dot within the red circles (1,000×) in all groups (except for the negative control). Scale bar=20 μm. (C) Body weight (n=5). (D) Serum creatinine (mg/dl) (n=5). (E) Serum blood urea nitrogen (BUN) (mg/dl) (n=5). The PC+NSS, PC+D-gal, and Box A+D-gal labels represent the control group, the kidney injury (D-gal) group, and the group pretreated with Box A in kidney injury (Box A), respectively. The values represent the means±SEMs. **p≤0.01, ***p≤0.001.*

Quantification of proinflammatory cytokines and DNA damage response gene expression in kidney tissues. The collected kidneys were kept in an RNA-preserving solution (RNA store reagent, Tiangen Biotech, Beijing, China) at 4˚C for three days and then at −20˚C until RNA extraction. The mRNA expression levels of tumor necrosis factor-alpha (TNF-α), interleukin 6 (IL-6), and $p16^{INK4A}$ were determined as described previously (25). In brief, the rat kidneys were homogenized in a Mini-Beadbeater (Biospec Products, Bartlesville, OK, USA). RNA was extracted using TRIzol Reagent (Invitrogen, Lidingo, Sweden), and DNase treatment was performed with a DNA removal and inactivation kit (Ambion, Life Technologies, Foster City, CA, USA). Then, the tissue RNA was converted to complementary DNA using reverse transcription reagents (Thermo Fisher Scientific). SYBR Green (Applied Biosystems)-based real-time PCR was then performed using the primers in Table II and analyzed with the comparative Ct method $^{(2-\Delta\Delta Ct)}$ as previously demonstrated (26). The mRNA expression levels of the target genes were normalized against the housekeeping gene GAPDH mRNA levels.

Statistics. Statistical analyses were performed with GraphPad Prism 9.4 (GraphPad Software, La Jolla, CA, USA). Student's *t*-tests were performed to compare the differences between the two groups for the experiments. Statistical significance was considered at $p<0.05$.

Results

Pretreatment with Box A prevented D-gal-induced alterations in serum creatinine and blood urea nitrogen. First, we administered Box A plasmid DNA to rats through intraperitoneal injection once a week (for 8 weeks). As a plasmid control (PC), pcDNA3.1 was employed. We subcutaneously injected D-gal into rats with kidney injury three days after the initial plasmid injection, while NSS was subcutaneously injected into the control group (daily for 8 weeks), as shown in Figure 1A. At the end of the study, we tracked plasmid delivery by monitoring the expression of the FLAG tag sequence by immunofluorescence staining. The results showed that the plasmid was delivered to the kidneys in all groups (except for the negative control) that contained plasmid transfection into the nucleus by the presence of a green dot within the red circles (Figure 1B). Our results demonstrated that the body weight of the rats was not different between the different groups (Figure 1C). Furthermore, D-gal induction significantly increased serum creatinine ($p<0.0000$) and serum blood urea nitrogen ($p=0.0013$) levels compared to the control levels (Figure 1D and E). However, Box A significantly prevented the changes in serum creatinine ($p=0.0012$) and tended to prevent the changes in serum BUN compared with those in the D-gal group (Figure 1D and E). In contrast, compared to the control group, the Box A group showed no significant differences in serum creatinine and BUN levels. These data indicated that pretreatment with Box A improved renal function in rats with D-gal-induced kidney injury.

Preventive effects of Box A against histopathological changes in the kidneys. To further observe the protective effects of Box A on histopathology, histological changes

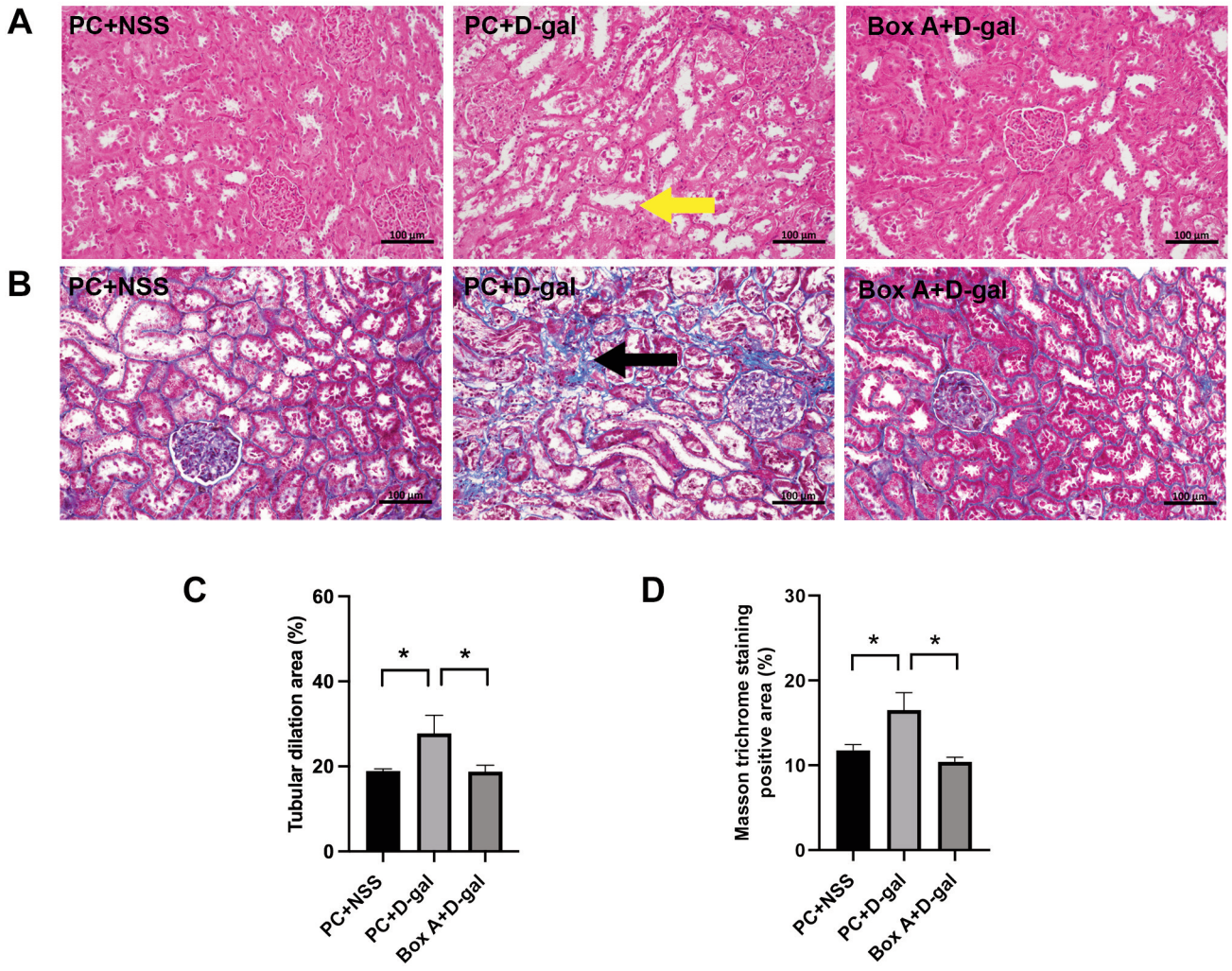

Figure 2. *Effects of Box A pretreatment on preventing cellular senescence-related histopathological changes in the kidneys. Histopathological examination of rat kidney tissue sections after eight weeks (H&E staining and Masson trichrome staining, 200×). Scale bar=100 µm. (A) Representative pictures of H&E staining in histological sections. The yellow arrow indicates the proximal renal tubular injury including tubular dilation with some areas representing karyolysis and thinned renal tubular epithelium. (B) Representative Masson trichrome staining pictures of histological sections. (C) The percentage of tubular dilation in histological sections (n=4) was calculated using Image J. (D) The percentage of positive area was analyzed to assess collagen accumulation (blue color, black arrow) in histological sections (n=4). The values represent the means±SEMs. *p≤0.05.*

related to tubular injury were quantified because senescence mainly affects the tubular structure. The D-gal group showed renal tubular injury including tubular epithelial damage and dilation with some areas representing karyolysis and thinned renal tubular epithelium as indicated in the yellow arrow in Figure 2A. However, the kidney injury defects were abolished by Box A pretreatment and the kidney resembled that of the control group. Moreover, the tubular dilation was calculated by estimating the proportion of tubules with tubule dilation. The results showed that the percentage of tubular dilation was significantly greater in the D-gal group than in the control (p=0.0408) and Box A (p=0.0452) groups (Figure 2A and C). Additionally, we used Masson trichrome staining to confirm the histopathological changes by measuring the collagen accumulation caused by cellular senescence-related kidney fibrosis. Our findings showed that the accumulation of collagen was significantly greater in the D-gal group than in the control (p=0.0369) and Box A (p=0.0149) groups (Figure 2B and D). However, Box A significantly prevented histopathological alterations caused by D-gal. Furthermore, compared to the control group, the Box A group showed no significant differences in any of the histopathological changes. These results indicate that Box A can prevent cellular senescence-related kidney diseases.

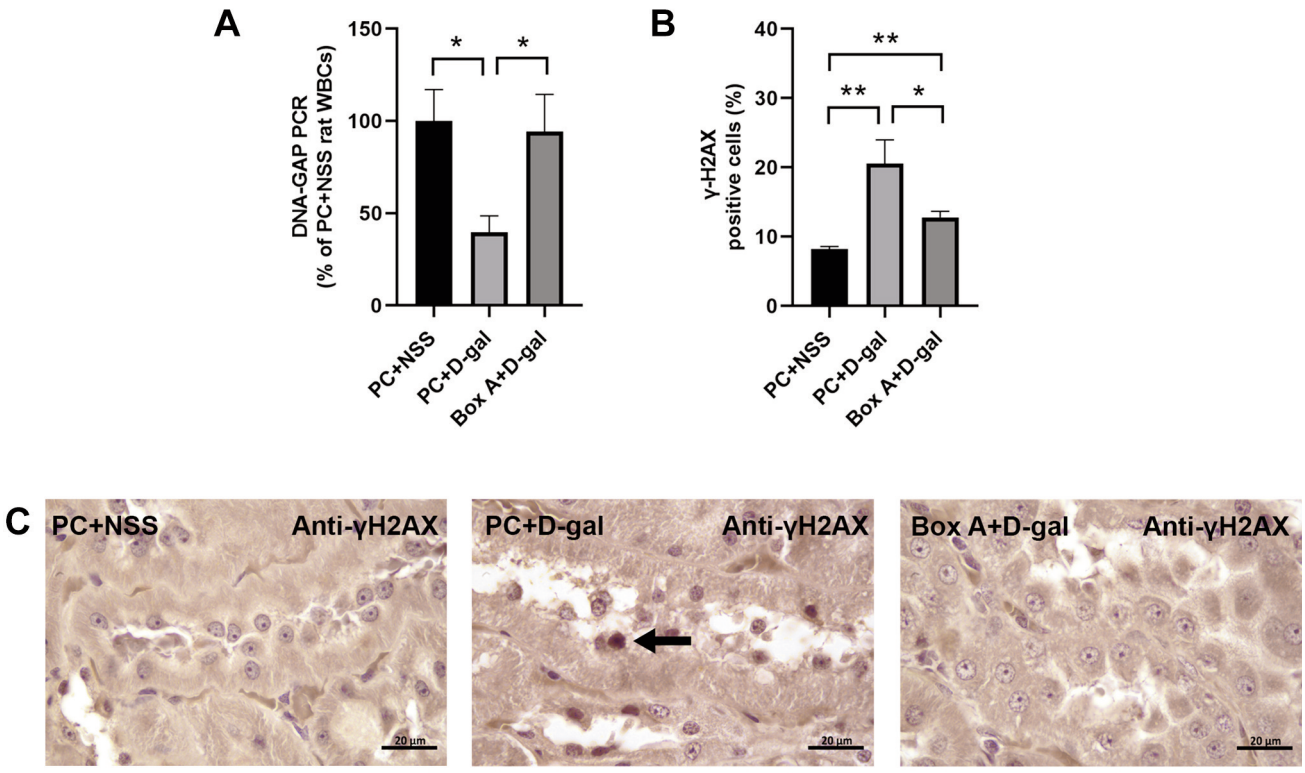

Figure 3. *Effects of pretreatment with Box A on maintaining DNA gaps and preventing DNA damage. (A) The DNA gaps (DNA-GAP number) were quantitated in rat white blood cells (WBCs; n=4) and was considered 100% in PC + NSS rat WBCs. (B) The percentage of DNA damage-positive cells was analyzed using γ-H2AX immunostaining in histological sections (n=4). (C) Representative photographs of γ-H2AX immunostaining in histological sections (1,000×). The black arrow indicates the positive area of γ-H2AX-positive cells. Scale bar=20 μm. The values represent the means±SEMs. *p≤0.05, and **p≤0.01.*

The preventive effects of Box A on DNA gap and DNA damage. We measured the number of epigenetic marks that prevent genomic instability, named DNA gaps, *via* DNA-GAP PCR. Our results demonstrated that the number of DNA gaps in the D-gal group was significantly lower than those in the control (p=0.0100) and Box A (p=0.0241) groups (Figure 3A). The percentage of DNA damage-positive cells with phosphorylation of the Ser-139 residue of the histone variant H2AX, forming γ-H2AX, was also significantly higher in the D-gal group than in the control (p=0.0061) and Box A (p=0.0360) groups (Figure 3B and C). However, Box A significantly prevented the reduction in DNA gaps and DNA damage. In addition, compared to the control group, the Box A group showed no significant difference in the alteration of the DNA gaps. The results suggested that Box A maintained DNA stability by preserving the DNA gap, preventing and the accumulation of DNA damage in rats with D-gal-induced kidney injury.

Pretreatment with Box A prevented cellular senescence in the kidneys. The persistence of a DNA damage response leads to the cellular senescence. Our results demonstrated that the D-gal accelerated kidney damage group exhibited significantly greater SA-beta-gal activity in the kidney tissues than the control (p=0.0033) and Box A (p=0.0066) groups (Figure 4A and C). Furthermore, we confirmed SA-beta-gal activity by detecting the mRNA expression of the senescent cell cycle arrest marker $p16^{INK4A}$. The results showed significantly greater mRNA expression of $p16^{INK4A}$ in the D-gal group than in the control (p=0.0377) and Box A (p=0.0118) groups (Figure 4B). Compared with D-gal, Box A significantly prevented the increases in SA-beta-gal staining and the mRNA expression of $p16^{INK4A}$ (Figure 4A-C). In addition, compared with the control group, the Box A group showed no significant difference in either SA-beta-gal activity or the mRNA expression of $p16^{INK4A}$. These findings indicated that Box A prevented kidney damage from irreversible cell cycle arrest in rats with D-gal-induced kidney injury.

Effects of Box A pretreatment on senescence-associated inflammatory responses in the kidneys. To further explore the role of Box A in preventing kidney damage, we investigated senescence-associated inflammatory responses. In kidney

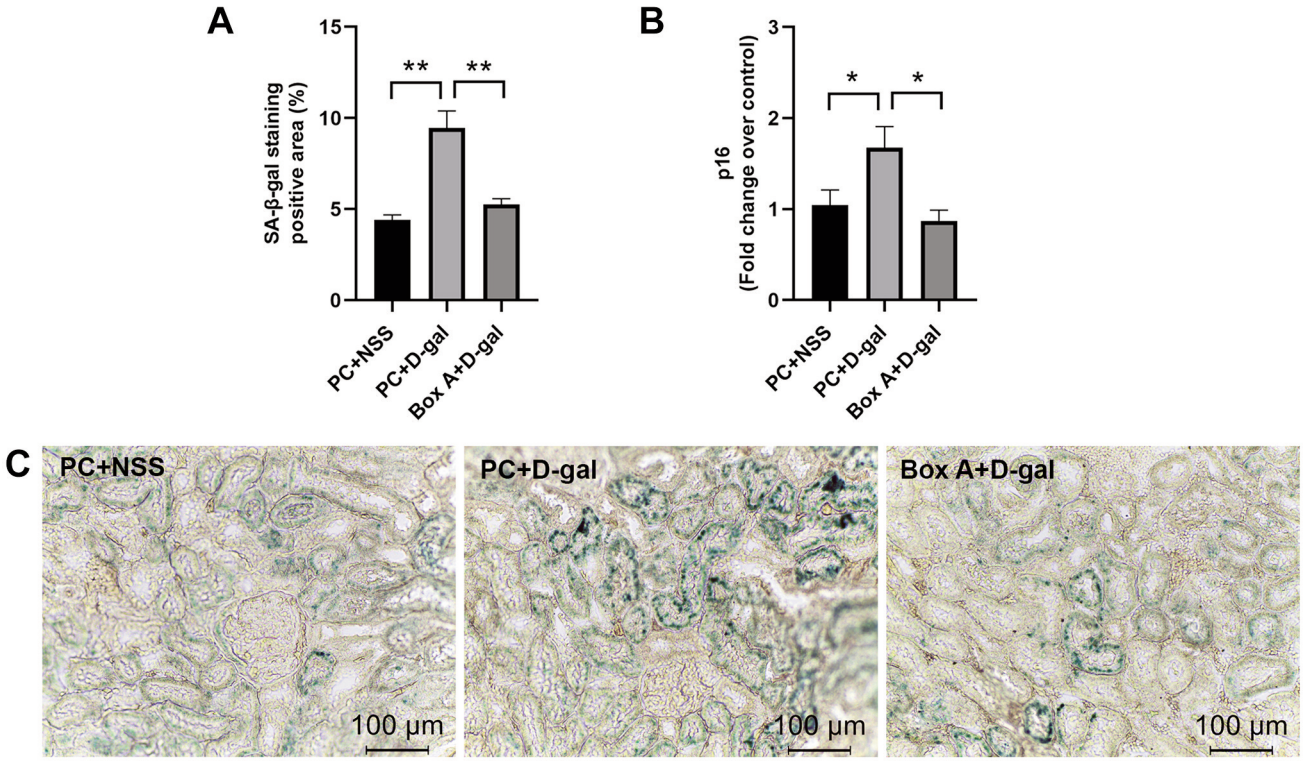

Figure 4. *Preventive effects of Box A on cellular senescence markers, including SA-beta-gal activity and p16^{INK4A} mRNA expression in rats with D-gal-induced kidney injury. (A) quantification of SA-beta-gal staining in rat kidney sections (n=3). (B) The mRNA expression of the p16^{INK4A} gene was identified via RNA-seq analysis (n=4). Total RNA was isolated from kidney rat tissues at the end of the study and used for RT-qPCR analysis of the indicated genes normalized to the housekeeping gene (GAPDH). (C) Representative pictures of SA-beta-gal staining in rat kidney sections (200×). Scale bar=100 μm. The values represent the means±SEMs. *p≤0.05, and **p≤0.01.*

sections in the D-gal group, the expression of the majority of senescence-associated secretory phenotype (SASP) regulators, including nuclear factor-κB (NF-κB), was significantly higher than that in the control (p=0.0329) and Box A (p=0.0314) groups (Figure 5A and D). In addition, we investigated the expression of NF-κB and detected the mRNA expression of related downstream SASP factors, including TNF-α and IL-6. The results showed that the mRNA expression of TNF-α and IL-6 was significantly greater in the D-gal group than in the control (p=0.0289 and p=0.0272, respectively) and Box A (p=0.0136 and p=0.0081, respectively) groups (Figure 5B and C). However, the relationship between NF-κB and the expression of the mRNA levels of TNF-α and IL-6 requires further assessment. Box A significantly prevented the increases in NF-κB expression and the mRNA expression of TNF-α and IL-6. In addition, compared to the control group, the Box A group showed no significant differences in protein and mRNA expression levels. These results suggested that Box A prevented senescent renal cells from exhibiting senescence-associated inflammatory responses by inhibiting SASP synthesis in rats with D-gal-induced kidney injury.

Discussion

Our study demonstrated that D-gal induction elevated serum creatinine and BUN; reduced DNA gaps; increased DNA damage in renal tubular cells; resulted in high positive SA-beta-gal staining; and resulted in overexpression of SASP factors, including NF-κB, TNF-α, and p16^{INK4A}. Furthermore, D-gal ultimately caused histopathological changes in the kidneys, namely, renal tubular dilation and kidney fibrosis. Interestingly, Box A plasmid administration prevented kidney damage in D-gal-induced kidney injury such that the Box A kidneys resembled the control kidneys. These results indicate that Box A administration ultimately prevents D-gal-induced kidney injury-mediated DNA damage and DDR in rats.

DNA damage and the associated DDR commonly cause renal injury (1). Recent studies also demonstrated evidence of cisplatin-induced cumulative DNA damage causing chronic kidney injury in mice (28). Similarly, previous studies have also shown that ischemia-reperfusion injury in the kidney is associated with DNA damage and DDR caused by excessive ROS (29). Sepsis also causes DNA damage and

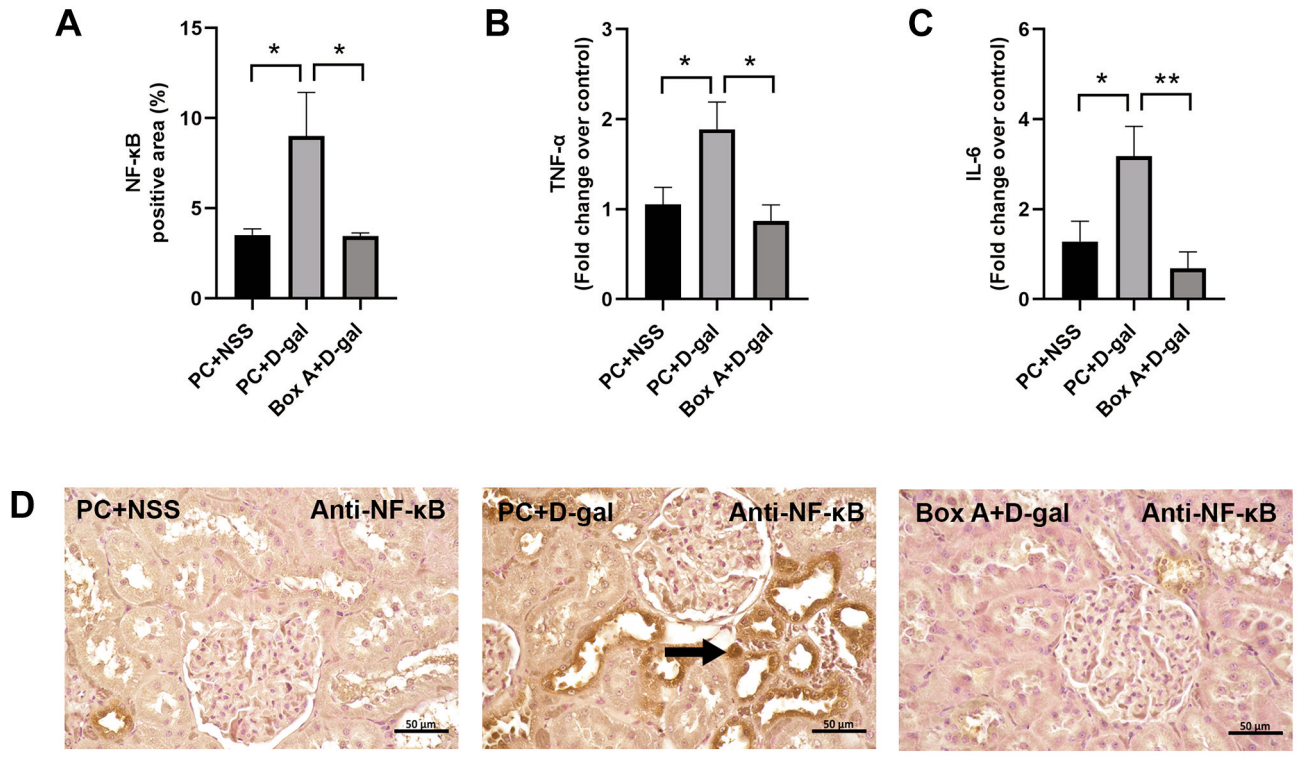

Figure 5. *Effects of Box A pretreatment on senescence-associated inflammatory responses in the kidneys. (A) The percentage of positive area was analyzed to assess NF-κB expression in histological sections (n=4) using immunohistochemistry. (B) mRNA expression of the TNF-α gene determined using RNA-seq analysis (n=4) in rat kidneys. (C) mRNA expression of the IL-6 gene determined using RNA-seq analysis (n=4) in rat kidneys. (D) Representative photographs of NF-κB immunostaining in histological sections (400×). Scale bar=50 μm. The black arrow indicates the positive area for immunostaining (brown color). The values represent the means±SEMs. *p≤0.05, and **p≤0.01.*

is consequently responsible for the pathogenesis of sepsis-induced acute kidney injury. The nuclear and mitochondrial DNA oxidation and damage have been demonstrated in sepsis-induced acute kidney injury (30). Exogenous and endogenous factors can damage DNA, including DNA oxidation, DNA hypomethylation, and reduction of youth-DNA-gap or RIND-EDSB, which ultimately cause genomic instability (15, 16, 31-33). Furthermore, cell cycle arrest is a physiological process of the DNA damage repair mechanism following injury (31). The genomic instability forces the cell to undergo cellular senescence with the persistence of a DDR (34). Thus, senescent cells are well known as sources of proinflammatory and profibrotic stimuli leading to increased oxidative stress, increased inflammation, and the creation of a vicious cycle involved in the pathological process of CKD (35-37).

According to our findings, D-gal significantly decreased DNA gaps and increased the formation of γ-H2AX DNA damage foci, which are known as early and sensitive markers of DNA damage and chromatin alteration that activate cell cycle arrest in a p53-dependent manner (38, 39). In addition, our results demonstrated that D-gal significantly elevated $p16^{INK4A}$ mRNA expression along with positive SA-beta-gal staining in kidney tissue sections, especially in renal tubular cells, which increased dramatically with tissue damage and age. These results are related to evidence that the most significant changes in the kidneys are found in renal tubular cells compared with other renal cell types (40). However, a marker of renal tubular injury, KIM-1, should be detected to confirm the injurious effect of D-gal on renal tubular injury, which could explain the increment of BUN level from D-gal induction. Moreover, SA-beta-gal staining is also widely used to determine senescence and detect the early development of morphologic lesions, in which cell senescence is involved during the pathogenesis of renal diseases (41, 42). Furthermore, our findings demonstrated that D-gal significantly elevated NF-κB activation and promoted inflammation through increased IL-6 and TNF-α levels, accelerating kidney tissue injury and fibrosis. These results are relevant to evidence that NF-κB has been well established as a pivotal mediator of inflammation in human patients with kidney diseases and animal models of renal inflammation and injury (43). Thus, D-gal induction decreases DNA gaps and causes reduced DNA durability,

leading to DNA damage, inflammation, and cellular senescence-related fibrosis in kidney tissues. Therefore, prevention of DNA gap reduction is a potential strategy for preventing kidney failure.

Our previous studies have reported that Box A acts as molecular scissor to produce DNA gaps to increase DNA durability (15). Loss of intranuclear HMGB1 results in HMGB1-produced DNA gap reduction leading to DNA damage and genome-wide hypomethylation (10, 15, 16). DDR can stimulate the senescence process responsible for inflammation, such as NF-κB and SASP (44). Extracellular HMGB1 promotes inflammation and, consequently, tissue damage (45-49). The loss of DNA protection role of intranuclear HMGB1 and the activation of inflammation process by extracellular HMGB1 may be associated with kidney tissue injury and fibrosis. Oxidative stress can promote the extracellular activities of HMBG1 by redox modification of the HMGB1 protein structure (50). The release mechanism is p53-dependent (51). Excessive oxidative stress in D-gal may cause HMGB1 release, and consequently, a low endogenous HMGB1-produced DNA gap and a high level of extracellular HMBG1.

On the contrary, our results demonstrated that Box A pretreatment prevents DNA gap reduction and the consequences of DNA damage and senescence from molecular to histopathology. This may be due to the limitation of DNA damage-activated p53-dependent HMGB1 release, and the post-translational modification of Box B and C terminal, which is required for HMGB1 release. Therefore, Box A and endogenous HMGB1 can stay intracellular, produce DNA gaps and prevent senescence due to oxidative stress conditions. Thus, Box A effectively prevented DNA damage-mediated kidney injury because Box A created DNA gaps and resisted the HMGB1 release process.

Conclusion

DNA gap reduction plays a crucial role in the molecular pathogenic process that promotes genomic instability by decreasing DNA durability and consequently increasing DNA damage in rats with D-gal-induced kidney injury. According to our findings, Box A can maintain DNA stability by preserving DNA gaps and preventing the accumulation of DNA damage, which is the consequence of the DDR that leads to cellular senescence-induced inflammation in rats with D-gal-induced kidney injury. Therefore, Box A is a promising therapeutic agent for ameliorating kidney injury.

Funding

This work was supported by Chulalongkorn University (The 100th Anniversary Chulalongkorn University for Doctoral Scholarship to Wilunplus Khumsri), the Ratchadapisek Somphot Fund for Postdoctoral Fellowship, Chulalongkorn University, and the National Science and Technology Development Agency, Thailand (Research Chair Grant, P-19-50189).

Conflicts of Interest

The Authors declare that there are no conflicts of interest in relation to this study.

Authors' Contributions

Conceptualization, WP, SY, and AM; methodology and investigation: WK, SY, and AK; writing-original draft, WK; writing-review and editing: WP, SY, and AM; visualization and supervision: WP, SY, NC, SC, and AM. The Authors have read and agreed to the published version of the manuscript.

Acknowledgements

The Authors thank the research staff of the Pathobiology department for supporting each technique performed in this research. The facilities are supported by the Pathobiology Information and Learning Center, Department of Pathobiology, Faculty of Science, Mahidol University, Bangkok, Thailand.

References

1 Wang P, Ouyang J, Jia Z, Zhang A, Yang Y: Roles of DNA damage in renal tubular epithelial cells injury. Front Physiol 14: 1162546, 2023. DOI: 10.3389/fphys.2023.1162546

2 Ling J, Ng JKC, Chan JCN, Chow E: Use of continuous glucose monitoring in the assessment and management of patients with diabetes and chronic kidney disease. Front Endocrinol (Lausanne) 13: 869899, 2022. DOI: 10.3389/fendo.2022.869899

3 Irazabal MV, Torres VE: Reactive oxygen species and redox signaling in chronic kidney disease. Cells 9(6): 1342, 2020. DOI: 10.3390/cells9061342

4 Liu CM, Ma JQ, Lou Y: Chronic administration of troxerutin protects mouse kidney against d-galactose-induced oxidative DNA damage. Food Chem Toxicol 48(10): 2809-2817, 2010. DOI: 10.1016/j.fct.2010.07.011

5 El-Far AH, Lebda MA, Noreldin AE, Atta MS, Elewa YHA, Elfeky M, Mousa SA: Quercetin attenuates pancreatic and renal D-galactose-induced aging-related oxidative alterations in rats. Int J Mol Sci 21(12): 4348, 2020. DOI: 10.3390/ijms21124348

6 Molitoris BA: DNA damage response protects against progressive kidney disease. J Clin Invest 129(11): 4574-4575, 2019. DOI: 10.1172/JCI131171

7 Kongruttanachok N, Phuangphairoj C, Thongnak A, Ponyeam W, Rattanatanyong P, Pornthanakasem W, Mutirangura A: Replication independent DNA double-strand break retention may prevent genomic instability. Mol Cancer 9: 70, 2010. DOI: 10.1186/1476-4598-9-70

8 Thongsroy J, Matangkasombut O, Thongnak A, Rattanatanyong P, Jirawatnotai S, Mutirangura A: Replication-independent endogenous DNA double-strand breaks in Saccharomyces cerevisiae model. PLoS One 8(8): e72706, 2013. DOI: 10.1371/journal.pone.0072706

9 Pongpanich M, Patchsung M, Thongsroy J, Mutirangura A: Characteristics of replication-independent endogenous double-strand breaks in Saccharomyces cerevisiae. BMC Genomics 15(1): 750, 2014. DOI: 10.1186/1471-2164-15-750

10 Thongsroy J, Patchsung M, Pongpanich M, Settayanon S, Mutirangura A: Reduction in replication□independent endogenous DNA double□strand breaks promotes genomic instability during chronological aging in yeast. FASEB J 32(11): 6252-6260, 2018. DOI: 10.1096/fj.201800218RR

11 Mutirangura A: Is global hypomethylation a nidus for molecular pathogenesis of age-related noncommunicable diseases? Epigenomics 11(6): 577-579, 2019. DOI: 10.2217/epi-2019-0064

12 Pornthanakasem W, Kongruttanachok N, Phuangphairoj C, Suyarnsestakorn C, Sanghangthum T, Oonsiri S, Ponyeam W, Thanasupawat T, Matangkasombut O, Mutirangura A: LINE-1 methylation status of endogenous DNA double-strand breaks. Nucleic Acids Res 36(11): 3667-3675, 2008. DOI: 10.1093/nar/gkn261

13 Ei ZZ, Mutirangura A, Arunmanee W, Chanvorachote P: The role of box A of HMGB1 in enhancing stem cell properties of human mesenchymal cells: a novel approach for the pursuit of anti-aging therapy. In Vivo 37(5): 2006-2017, 2023. DOI: 10.21873/invivo.13298

14 Thongsroy J, Mutirangura A: The inverse association between DNA gaps and HbA1c levels in type 2 diabetes mellitus. Sci Rep 13(1): 18987, 2023. DOI: 10.1038/s41598-023-46431-2

15 Yasom S, Watcharanurak P, Bhummaphan N, Thongsroy J, Puttipanyalears C, Settayanon S, Chalertpet K, Khumsri W, Kongkaew A, Patchsung M, Siriwattanakankul C, Pongpanich M, Pin-On P, Jindatip D, Wanotayan R, Odton M, Supasai S, Oo TT, Arunsak B, Pratchayasakul W, Chattipakorn N, Chattipakorn S, Mutirangura A: The roles of HMGB1-produced DNA gaps in DNA protection and aging biomarker reversal. FASEB Bioadv 4(6): 408-434, 2022. DOI: 10.1096/fba.2021-00131

16 Watcharanurak P, Mutirangura A: Human RNA-directed DNA methylation methylates high-mobility group box 1 protein-produced DNA gaps. Epigenomics 14(12): 741-756, 2022. DOI: 10.2217/epi-2022-0022

17 Swaminathan S, Tomkinson B, Kieff E: Recombinant Epstein-Barr virus with small RNA (EBER) genes deleted transforms lymphocytes and replicates *in vitro*. Proc Natl Acad Sci U.S.A. 88(4): 1546-1550, 1991. DOI: 10.1073/pnas.88.4.1546

18 Gao Q, Chen F, Zhang L, Wei A, Wang Y, Wu Z, Cao W: Inhibition of DNA methyltransferase aberrations reinstates antioxidant aging suppressors and ameliorates renal aging. Aging Cell 21(1): e13526, 2022. DOI: 10.1111/acel.13526

19 Humphreys BD: Mechanisms of renal fibrosis. Annu Rev Physiol 80(1): 309-326, 2018. DOI: 10.1146/annurev-physiol-022516-034227

20 Docherty MH, O'Sullivan ED, Bonventre JV, Ferenbach DA: Cellular senescence in the kidney. J Am Soc Nephrol 30(5): 726-736, 2019. DOI: 10.1681/ASN.2018121251

21 Tang C, Livingston MJ, Liu Z, Dong Z: Autophagy in kidney homeostasis and disease. Nat Rev Nephrol 16(9): 489-508, 2020. DOI: 10.1038/s41581-020-0309-2

22 Tominaga T, Shimada R, Okada Y, Kawamata T, Kibayashi K: Senescence-associated-β-galactosidase staining following traumatic brain injury in the mouse cerebrum. PLoS One 14(3): e0213673, 2019. DOI: 10.1371/journal.pone.0213673

23 Pan H, Feng W, Chen M, Luan H, Hu Y, Zheng X, Wang S, Mao Y: Alginate oligosaccharide ameliorates D-galactose-induced kidney aging in mice through activation of the Nrf2 signaling pathway. Biomed Res Int 2021: 6623328, 2021. DOI: 10.1155/2021/6623328

24 Balhorn R, Hartmann C, Schupp N: Aldosterone induces DNA damage and activation of Nrf2 mainly in tubuli of mouse kidneys. Int J Mol Sci 21(13): 4679, 2020. DOI: 10.3390/ijms21134679

25 Peinnequin A, Mouret C, Birot O, Alonso A, Mathieu J, Clarençon D, Agay D, Chancerelle Y, Multon E: Rat pro-inflammatory cytokine and cytokine related mRNA quantification by real-time polymerase chain reaction using SYBR green. BMC Immunol 5: 3, 2004. DOI: 10.1186/1471-2172-5-3

26 Schmittgen TD, Livak KJ: Analyzing real-time PCR data by the comparative CT method. Nat Protoc 3(6): 1101-1108, 2008. DOI: 10.1038/nprot.2008.73

27 Pascale RM, Simile MM, De Miglio MR, Muroni MR, Calvisi DF, Asara G, Casabona D, Frau M, Seddaiu MA, Feo F: Cell cycle deregulation in liver lesions of rats with and without genetic predisposition to hepatocarcinogenesis. Hepatology 35(6): 1341-1350, 2002. DOI: 10.1053/jhep.2002.33682

28 Yamashita N, Nakai K, Nakata T, Nakamura I, Kirita Y, Matoba S, Humphreys BD, Tamagaki K, Kusaba T: Cumulative DNA damage by repeated low-dose cisplatin injection promotes the transition of acute to chronic kidney injury in mice. Sci Rep 11(1): 20920, 2021. DOI: 10.1038/s41598-021-00392-6

29 Yan M, Tang C, Ma Z, Huang S, Dong Z: DNA damage response in nephrotoxic and ischemic kidney injury. Toxicol Appl Pharmacol 313: 104-108, 2016. DOI: 10.1016/j.taap.2016.10.022

30 van der Slikke EC, Star BS, van Meurs M, Henning RH, Moser J, Bouma HR: Sepsis is associated with mitochondrial DNA damage and a reduced mitochondrial mass in the kidney of patients with sepsis-AKI. Crit Care 25(1): 36, 2021. DOI: 10.1186/s13054-020-03424-1

31 Jackson SP, Bartek J: The DNA-damage response in human biology and disease. Nature 461(7267): 1071-1078, 2009. DOI: 10.1038/nature08467

32 Cooke MS, Evans MD, Dizdaroglu M, Lunec J: Oxidative DNA damage: mechanisms, mutation, and disease. FASEB J 17(10): 1195-1214, 2003. DOI: 10.1096/fj.02-0752rev

33 Ehrlich M: DNA hypomethylation in cancer cells. Epigenomics 1(2): 239-259, 2009. DOI: 10.2217/epi.09.33

34 Branzei D, Foiani M: Regulation of DNA repair throughout the cell cycle. Nat Rev Mol Cell Biol 9(4): 297-308, 2008. DOI: 10.1038/nrm2351

35 Wang WJ, Cai GY, Chen XM: Cellular senescence, senescence-associated secretory phenotype, and chronic kidney disease. Oncotarget 8(38): 64520-64533, 2017. DOI: 10.18632/oncotarget.17327

36 Xu J, Zhou L, Liu Y: Cellular senescence in kidney fibrosis: pathologic significance and therapeutic strategies. Front Pharmacol 11: 601325, 2020. DOI: 10.3389/fphar.2020.601325

37 Zhao JL, Qiao XH, Mao JH, Liu F, Fu HD: The interaction between cellular senescence and chronic kidney disease as a therapeutic opportunity. Front Pharmacol 13: 974361, 2022. DOI: 10.3389/fphar.2022.974361

38 Turinetto V, Giachino C: Multiple facets of histone variant H2AX: a DNA double-strand-break marker with several biological functions. Nucleic Acids Res 43(5): 2489-2498, 2015. DOI: 10.1093/nar/gkv061

39 Lanz MC, Dibitetto D, Smolka MB: DNA damage kinase signaling: checkpoint and repair at 30 years. EMBO J 38(18): e101801, 2019. DOI: 10.15252/embj.2019101801

40 Melk A, Schmidt BM, Takeuchi O, Sawitzki B, Rayner DC, Halloran PF: Expression of p16INK4a and other cell cycle regulator and senescence associated genes in aging human kidney. Kidney Int 65(2): 510-520, 2004. DOI: 10.1111/j.1523-1755.2004.00438.x

41 Valieva Y, Ivanova E, Fayzullin A, Kurkov A, Igrunkova A: Senescence-associated β-galactosidase detection in pathology. Diagnostics (Basel) 12(10): 2309, 2022. DOI: 10.3390/diagnostics12102309

42 Li Z, Wang Z: Aging kidney and aging-related disease. Adv Exp Med Biol 1086: 169-187, 2018. DOI: 10.1007/978-981-13-1117-8_11

43 Zhang H, Sun SC: NF-κB in inflammation and renal diseases. Cell Biosci 5: 63, 2015. DOI: 10.1186/s13578-015-0056-4

44 Yue Z, Nie L, Zhao P, Ji N, Liao G, Wang Q: Senescence-associated secretory phenotype and its impact on oral immune homeostasis. Front Immunol 13: 1019313, 2022. DOI: 10.3389/fimmu.2022.1019313

45 Wang L, Botchway BOA, Liu X: The repression of the HMGB1-TLR4-NF-κB signaling pathway by safflower yellow may improve spinal cord injury. Front Neurosci 15: 803885, 2021. DOI: 10.3389/fnins.2021.803885

46 Yang H, Tracey KJ: Targeting HMGB1 in inflammation. Biochim Biophys Acta 1799(1-2): 149-156, 2010. DOI: 10.1016/j.bbagrm.2009.11.019

47 Fonken LK, Frank MG, Kitt MM, D'Angelo HM, Norden DM, Weber MD, Barrientos RM, Godbout JP, Watkins LR, Maier SF: The alarmin HMGB1 mediates age-induced neuroinflammatory priming. J Neurosci 36(30): 7946-7956, 2016. DOI: 10.1523/JNEUROSCI.1161-16.2016

48 Yang H, Lundbäck P, Ottosson L, Erlandsson-Harris H, Venereau E, Bianchi ME, Al-Abed Y, Andersson U, Tracey KJ: Redox modifications of cysteine residues regulate the cytokine activity of HMGB1. Mol Med 27(1): 58, 2021. DOI: 10.1186/s10020-021-00307-1

49 Chen Q, Guan X, Zuo X, Wang J, Yin W: The role of high mobility group box 1 (HMGB1) in the pathogenesis of kidney diseases. Acta Pharm Sin B 6(3): 183-188, 2016. DOI: 10.1016/j.apsb.2016.02.004

50 Ferrara M, Chialli G, Ferreira LM, Ruggieri E, Careccia G, Preti A, Piccirillo R, Bianchi ME, Sitia G, Venereau E: Oxidation of HMGB1 is a dynamically regulated process in physiological and pathological conditions. Front Immunol 11: 1122, 2020. DOI: 10.3389/fimmu.2020.01122

51 Davalos AR, Kawahara M, Malhotra GK, Schaum N, Huang J, Ved U, Beausejour CM, Coppe JP, Rodier F, Campisi J: p53-dependent release of Alarmin HMGB1 is a central mediator of senescent phenotypes. J Cell Biol 201(4): 613-629, 2013. DOI: 10.1083/jcb.201206006

Received February 1, 2024
Revised February 29, 2024
Accepted March 1, 2024